International Journal of Physics and Applications
Online ISSN: 2664-7583; Print ISSN: 2664-7575
Received: 01-11-2018; Accepted: 02-12-2018; Published: 02-01-2019
www.physicsjournal.in
Volume 1; Issue 1; 2019; Page No. 01-10

The estimation of solar cell parameters and the pursuit of maximum power through voltage-current characteristic using ant colony Algorithm

Hossein Gholipour-Goudarzi[1], Hossein Asgharpour-Alamdari[2*]
[1-2] Faculty of Electrical and Computer Engineering, Technical and vocational University, Babol (Imam Sadegh) University, Iran

DOI: https://doi.org/10.33545/26647575.2019.v1.i1a.13

Abstract
In this paper, the ant colony algorithm has been used to find single and two-diode models of solar cells, and then to calculate the maximum power point of photovoltaic cells. First, it is tried to find an exact model of the solar cell by the ant colony algorithm and then to track the maximum power point by the use of the direct method. To verify the results of the simulation and to examine the accuracy of the proposed algorithm, the results of this algorithm have been compared with the ones obtained from algorithms in other sources. They indicate that the ACO algorithm has a higher accuracy than other methods and the error of the model proposed by this algorithm is so negligible. After finding single and two-diode models of solar cells, these two have been applied to track the maximum power point of the solar cell and a comparison has been made among the maximum powers achieved by each these two models.

Keywords: solar cell, colony algorithm, optimization, voltage-current characteristic

1. Introduction
The increasing demand for electricity from the consumers and the growing environmental pollution have made researchers think of a way to reduce emissions. One of these methods is the use of solar energy. Many nations are doing their best to replace solar energy with old energy sources in producing energy and electricity to make the most use of this kind of energy source and to reduce the damages caused by fossil fuels. Finding a solar cell model is very important, because the first step to simulating, controlling, evaluating performance, designing and optimizing solar cells is to have an exact model of it. Now, the more precise the presented model is, the more accurate the calculations and the closer the simulation results to the results obtained in reality will be. The characteristics of PV (photovoltaic) systems are inherently nonlinear and they follow environmental parameters such as the radiation rate, the ambient temperature and the electric load related to it. Therefore, by the right choice of operating point of photovoltaic array, the maximum power of the PV array can be obtained when the radiation and the temperature are constant [1]. The initial start-up costs and the low efficiency of energy conversion are among the disadvantages of using photovoltaic systems. Lots of efforts have been made to alleviate the above disadvantages and to increase the energy conversion efficiency by enhancing the quality of solar cells and getting the maximum power from solar cells. With changes in environmental conditions (radiation and temperature), the operating point of arrays changes, and consequently, by the use of different algorithms tracking the maximum power point, the amount of power received from the array can always be kept at its maximum value, or, in other words, the maximum power point can be tracked. There are several methods to track the maximum power. The most important of these include: Hill-Climbing, P&O [1], incremental conductance, fuzzy logic control, the parasitic capacitance, Ripple control and. [4, 8]. One of the methods to track the maximum power point is the direct method. In this method, first a precise model of the solar cell is introduced and then with respect to the temperature and light intensity, the derivative of the following solar cell power equation is found and its extreme point can be obtained or the Newton method can be applied to track the maximum power point of the solar cell rather than finding its derivative [9]. Since the solar cell characteristic (current-voltage curve) is strongly nonlinear, determining the unknown parameters of the system using the current classical approaches seems not possible anymore and it causes the emergence of smart algorithms. Several algorithms have been used to determine the parameters of a solar cell, and all had the problem being stopped in local optimum points. In addition, some algorithms had low convergence or sometimes were even divergent in determining the parameters of solar cells. Therefore, an algorithm characterized by both high convergence speed and accuracy should be offered in order not to be stopped in local optimum points [10]. In this paper, the ant colony algorithm has been used to obtain a solar cell model and to track the maximum power point of photovoltaic cells. The ant colony algorithm has a high convergence capability causing it not to be stopped in local optimum points, suitable for resolving such these problems. At the beginning, it is intended to find a precise model of the solar cell by the ant colony algorithm and then to track the maximum power point using the direct method. Later in the second section, the solar cell model and its equations are presented. In section 3, the ant colony

[1]. Perturb & Observe

algorithm will be described in brief and then in the fourth section, the results of simulation are illustrated. The paper ends in part 5 producing some results.

2. The Electric Models of Solar Cells

An ideal solar cell is modeled by a current source (generated by light) parallel with a reverse diode. In figure 1, the ideal model of a solar cell is shown, but in practice it is observed that the results of testing do not fully correspond with this model. As a result, by making some changes in the real model, we use mathematical models.

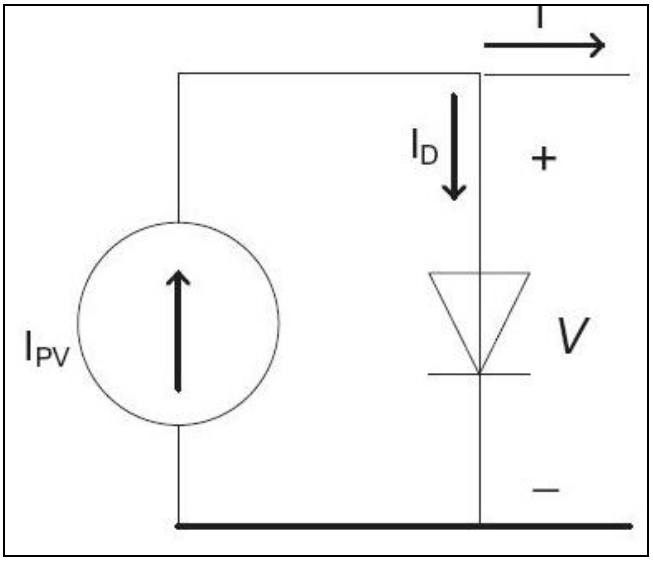

Fig 1: The Ideal Solar Cell Model

Many mathematical models have been introduced to describe the I-V nonlinear curve of the solar cell. But these models can be limited into two common models. The single–diode model and the two-diode model. Because of their simplicity and high precision, these two models have drawn the attention of many researchers and are the most common solar cell models. Therefore, these two models are brought into use in this paper [11].

2.1 The Single-Diode Model

As shown in figure 2, the single-diode model is more simple and closer to the ideal model which has made it more common than other models. In this model, the currents of two diodes are combined. It seems this model is of less precision compared with the two-diode model, but in practice, we see that, because of its simplicity and high speed to reach the final answer, this model is given more attention and researchers try to study the experimental data with I-V curve of the solar cell according to this model. [12] The equation of the terminal current of this model could then be presented as follows.

$$I_t = I_{ph} - I_{sd}\left[\exp\left(\frac{q(V_t - R_s I_t)}{nkT}\right) - 1\right] - \frac{V_t + R_s I_t}{R_{sh}} \quad (1)$$

Where V represents the voltage, It is the output photovoltaic current, q is the electric load, Iph is the flow generated by the solar array, $I_{s1,2}$ is the saturation current of the diodes, $n_{1,2}$ is the ideal coefficient of the link of the diodes D1 and D2, K is the Boltzmann's constant, and T is the cell temperature. The unknown parameters to be achieved have been reduced to five ones Rs ، Rsh ، Iph ، Isd and n.

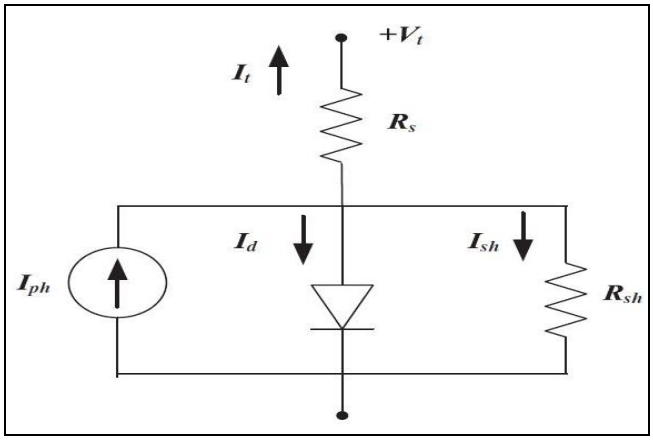

Fig 2: The Single-Diode Model of the Solar Cell

2.2 The Two-Diode Model

Let's consider the model to be studied with two diodes. This model, as shown in figure 3, actually includes the different internal resistances of the photovoltaic cell. The model includes the current source Iph, which models the conversion of the radiant energy into electrical current. Parallel resistance Rsh represents the leakage resulted from some externalities on photovoltaic cells, the series resistance Rs shows the variable resistances of connections, and parallel diodes D1 and D2 represent the PN link model [13].

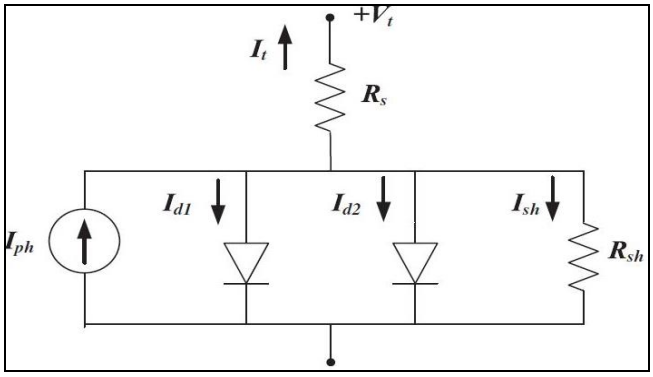

Fig 3: The Model of Photovoltaic Cell with Two Diodes

The current produced by the module is as the following equation:

$$I_t = I_{ph} - I_{d1} - I_{d2} - I_{sh} \quad (2)$$

$$I_t = I_{ph} - I_{sd1}\left[\exp\left(\frac{q(V_t + R_s I_t)}{n_1 kT}\right) - 1\right] - I_{sd2}\left[\exp\left(\frac{q(V_t + R_s I_t)}{n_2 kT}\right) - 1\right] - \frac{V_t + R_s I_t}{R_{sh}} V_t \quad (3)$$

t is clear from equation (3) that the output current of photovoltaic modules depends on the radiant flow and the flow itself depends on solar radiation and the temperature of

the junction of module cells. In the same way, the power that a module can transmit depends on the solar radiation and the temperature of semiconductor conjunction. Here Isd1 and Isd2 represent the discharge and saturation currents of the first and second diodes, Vt is the voltage across the terminals, and Rs and Rsh are the parallel and series resistances. q Shows the electric load, K is the Boltzmann constant, n1 and n2 are the ideal coefficient of diodes, and T is the temperature at which the experiment was performed the unit of which is "ok".
Having the test temperature and measuring the voltage and the output current of the terminal, seven other parameters remain unknown. By using an optimization technique and with the help of the data obtained from the experiment, the above unknown parameters can be found.

3. A General Overview of the Optimization Method

The issue is finding the unknown parameters of solar cells. The unknown parameters or the algorithm variables can be separated for both single and two-diode models in the relations (4) and (5) below.

$$x = [R_s \;\; R_{sh} \;\; I_{ph} \;\; I_{sd} \;\; n] \tag{4}$$

$$x = [R_s \;\; R_{sh} \;\; I_{ph} \;\; I_{sd1} \;\; I_{sd2} \;\; n_1 \;\; n_2] \tag{5}$$

In many articles and studies in this regard, different bounds have been introduced for the parameters above [14]. But the most common upper and lower bounds used in the case of solar cell parameters are as follows:

Table 1: The Scope of the Unknown Parameters of Solar Cells

Parameter	Lower	Upper
$R_s(\Omega)$	0	0.5
$R_{sh}(\Omega)$	0	100
$I_{ph}(A)$	0	1
$I_{sd}(\mu A)$	0	1
N	1	2

3.1 The Objective Function

To achieve the objective function, the relations 6 and 7 are respectively used for the single and two-diode models [15]:

$$f(V_t, I_t, x) = I_t - I_{ph} + I_{sd}\left[\exp\left(\frac{q(V_t + R_s I_t)}{nkT}\right) - 1\right] + \frac{V_t + R_s I_t}{R_{sh}} \tag{6}$$

$$f(V_t, I_t, x) = I_t - I_{ph} + I_{sd1}\left[\exp\left(\frac{q(V_t + R_s I_t)}{n_1 kT}\right) - 1\right] + I_{sd2}\left[\exp\left(\frac{q(V_t + R_s I_t)}{n_2 kT}\right) - 1\right] \tag{7}$$

Now, if we replace the amounts of voltage and current obtained from the real experiment and the amount of the specific parameters which are shown in relations 6 and 7 in the algorithm, then, the function $f(V_t, I_t, x)$ shows the amount of computational error between the actual testing results and the results of the algorithm. And if the number of actual results is N, then there will be N errors for an algorithm output.
q is the electron load, T is the temperature of the solar cell in Kelvin scale and K is Boltzmann's constant, the values of which are in the table (2):

Table 2: The Constant Values in Solar Cell Relations

q (c)	1.602e-19
T (^{o}k)	306
K	1.380650e-23

Using equations 6 and 7, we can obtain the values of errors in a variety of experiments for a series of solar cell parameters. This means that if we put some specific values instead of some unknown parameters of solar cells, there will be f practical tests (practical results) which make it possible to know whether the result obtained is desirable or not using the square root of the sum of squared errors [16]. The RMSE relation will be as follows:

$$RMSE = \sqrt{\frac{1}{N}\sum_{i=1}^{N}(f_i(V_t, I_t, x))^2} \tag{8}$$

Where N is the number of tests or the number of voltage and output current samples of the solar cell. In general, it can be said that for each series of parameters of the solar cell which has less RMSE, the values obtained for voltage and current from the algorithm will be closer to the terminal voltage and current of the solar cell obtained from the actual test. So the equation 8 can be accepted as an objective function and the purpose of the algorithm is to minimize this function.

4. The Ant Colony Optimization Algorithm

Ant colony optimization algorithm, briefly ACO or Optimization of Ant Colony is based on the actual movement of ants in nature initially proposed by Marco Dorigo in 1992 [17] in his PhD thesis which was first known as ant system. This behavior of ants is more for ensuring the survival of their colony. By conducting a detailed study in the behavior of ants and undertaking necessary practical reviews, it was concluded that ants (initially) wander randomly in the natural world, and upon finding food return to their colony while laying down pheromone trails. Ants are able to detect the existence of pheromone by their sense of smell. If other ants find such a path, they are likely not to keep travelling at random, but instead to follow the trail, returning and reinforcing it if they eventually find food. Over time, however, the pheromone trail starts to evaporate, thus reducing its attractive strength. The more time it takes for an ant to travel down the path and back again, the more time the pheromones have to evaporate. A short path, by comparison, gets marched over more frequently, and thus the pheromone density becomes higher on shorter paths than longer ones. Pheromone evaporation also has the advantage of avoiding the convergence to a locally optimal solution. If there were no evaporation at all, the paths chosen by the first ants would tend to be excessively attractive to the following ones. In that case, the exploration of the solution space would be constrained.
Thus, when one ant finds a good (i.e., short) path from the colony to a food source, other ants are more likely to follow that path, and positive feedback eventually leads to all the ants following a single path. The idea of the ant colony algorithm is to mimic this behavior with "simulated ants" walking

around the graph representing the problem to solve. Then, according to the features listed for ants, we are to study the structure of ACO algorithm [17].

4.1 The Structure of the Ant Colony Algorithm

An ACO problem can be described as follows:

Suppose there are N ants is an ant colony. According to figure (4), ants have started to move away from their nest. In each iteration or period, each ant takes a path from the first to the last layer with the goal of getting to its goal (food). Each ant in each layer can only choose one option with the probability of P_{ij} according to the following equation.

$$P_{ij}{}^{K} = \begin{cases} \dfrac{(\tau_{ij})^{\alpha}}{\sum_{j \in Ni}(\tau_{ij})^{\alpha}} & if\ j \in Ni \\ 0 & if\ j \nexists Ni \end{cases} \qquad (9)$$

τ_{ij} is the pheromone density left in the ij^{th} path, α shows the importance of pheromone, N_i is the number of neighboring places for the k^{th} ant, and j is the next location of the k^{th} ant. At the beginning of the optimization process all paths have an initial pheromone density. As shown in figure 4, ants have started to move away from their nests and randomly seek a value for the variable in each layer. With each iteration, each ant will take a solution vector (the path traveled by the ant) which consists of search variables between the nest and the food. This search will go on until the maximum repetition. The value of each variable will be selected as the optimal component of the solution vector based on the path that has had the highest pheromone density. And finally, in the optimal solution, almost all ants have chosen the best path which has the highest concentration of pheromone. The k^{th} ant, when being in location i, uses a τ_{ij} amount of pheromone to choose the next location (the j^{th} location). The probability of selecting each location will be calculated by relation (9). Selected points along the route traveled by each ant are the candidates for the problem solution. For example, a path taken by the k^{th} ant is highlighted in figure 4 and the points x_{12} ،x_{23} ،x_{31} ،x_{45} ،x_{56} ،x_{64} will make a full path between the nest and the food source. Formula (10) shows the rise in pheromone density after each ant's passage between locations i and j [18].

When the kth ant is taking a path, the amount of pheromone in all paths is evaluated using the following formula:

$$\tau_{ij}{}^{(k)} \leftarrow \tau_{ij}{}^{(k-1)} + \Delta\tau^{(k)} \qquad (10)$$

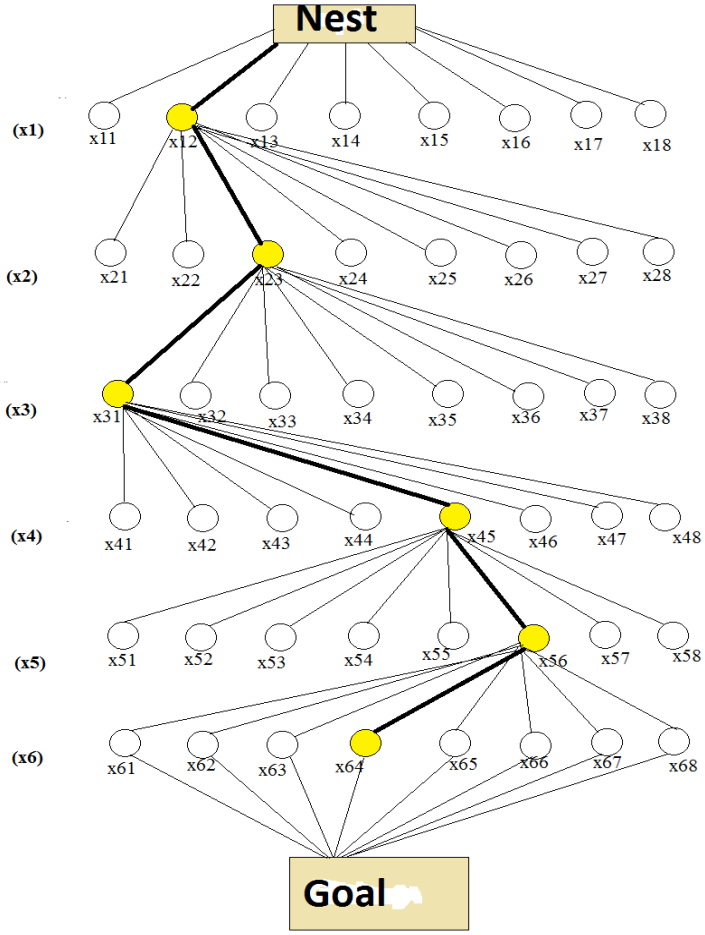

Fig 4: How Ants find the Path between the Nest and the Food Source in a Multivariate Problem

$$\tau_{ij} \leftarrow (1-\rho)\tau_{ij} \qquad \forall (i,j) \in A \tag{11}$$

Where ρ is the evaporation coefficient, a value within the interval (0, 1). A shows the paths taken from the nest to the food source. Taking the evaporation coefficient into account leads to the removal of too week responses and it will cause the search process to become dynamic, because there may be some other shorter paths. An iteration of the search process includes the ants' motion, pheromone evaluation and the amount of pheromone left. After all the ants return to their nest, the pheromone trails are updated by the following equation (12), and Where $\Delta\tau_{ij}^{(k)}$ is the amount of pheromone deposited on the arc ij by the superior ant k. The pheromone left by the best ant on the path ij can be obtained as follows equation (13) and where Q is a constant amount and Lk is the kth ant's tour (length). Equation (13) can be implemented as follows:

$$\tau_{ij} = (1-\rho)\tau_{ij} + \sum_{k=1}^{N} \Delta\tau_{ij}^{(k)} \tag{12}$$

$$\Delta\tau_{ij}^{(k)} = \frac{Q}{L_k} \tag{13}$$

Where f_{worst} is the worst and f_{best} is the best amount of the objective function among the tours taken by N ants, and ב is a parameter to control the global updating scale of pheromone. The larger this amount is, the more pheromone will be deposited on the best path and the better algorithm will be sought in the local optimizations. Then the actual optimization will be found and there will be no stoppage in the local optimizations.

5. The Simulation Results

In this part of the article, the results of the modeling are to be studied. For this purpose, first the single and then the two-diode models of solar cells are modeled, and then by the help from the ant colony algorithm, the precise parameters of solar cell models are determined. To confirm the results obtained from the simulation by the proposed algorithm, the results have been compared with some other algorithms as well. After finding the precise models of single and two-diode models of solar cells, these models have been used to track the maximum power of the solar cell. For this, in different radiations and at various temperatures, the maximum power values of the solar cell have been obtained.

5.1 The Characteristics of the Solar Cells Studied

The solar cell used in this article is a standard model (57 mm diameter commercial (R.T.C. France) silicon solar cell)- the one frequently used in articles to carry out modeling studies on solar cells. The results of the measurements of the real solar cell including its voltage and current in the radiation (1000 W / m2) and at a temperature of 33 °C are summarized in table 3 [19]. To gain more precise results, 26 various samplings have been done.

Table 3: The Results of the Measurement [19]

No.	1	2	3	4	5	6	7	8	9
Voltage (V)	-0.2057	-0.1291	-0.0588	0.0057	0.0646	0.1185	0.1678	0.2132	0.2545
Current (I)	0.7640	0.7620	0.7605	0.7605	0.7600	0.7590	0.7570	0.7570	0.7555
No.	10	11	12	13	14	15	16	17	18
Voltage (V)	0.2924	0.3269	0.3585	0.3873	0.4137	0.4373	0.4590	0.4784	0.4960
Current (I)	0.7540	0.7505	0.7465	0.7385	0.7280	0.7065	0.6755	0.6320	0.5730
No.	19	20	21	22	23	24	25	26	
Voltage (V)	0.5119	0.5265	0.5398	0.5521	0.5633	0.5736	0.5833	0.5900	
Current (I)	0.4990	0.4130	0.3165	0.2120	0.1035	-0.0100	-0.1230	-0.2100	

5.2 Optimization of the Single-Diode Solar Cells

In this part, the results achieved by optimizing the single-diode model of solar cells are presented. For this, the ant colony algorithm has been implemented 20 times and the best response has been recorded for further studies. The results obtained by different algorithms and also the proposed ant colony algorithm are summarized in table 4.

Table 4: The Comparison of the Results of Different Algorithms in the Single-Diode Solar Cells

	R_s	R_{sh}	I_{ph}	I_{sd}	N	RMSE
HS	0.0366	53.5946	0.7607	0.3049	1.4753	9.95e-04
GGHS	0.0363	53.0647	0.7609	0.3262	1.4821	9.91e-04
IGHS	0.3613	53.2845	0.7607	0.3435	1.4874	9.93e-04
SA	0.0345	43.1034	0.7621	0.4798	1.5172	1.90e-02
PS	0.0313	64.1026	0.7617	0.9981	1.6	1.49e-02
GA	0.0299	42.3729	0.7619	0.8087	1.5751	1.91e-02
PSO	0.0344	74.2264	0.7604	0.5239	1.5321	1.36e-03
ABC	0.0364	55.6547	0.7601	0.3064	1.48	11.06e-4
ACO	0.0324	53.2564	0.7457	0.3041	1.48	9.84e-4

According to the results in table 4, it can be said that the ant colony algorithm (ACO), with the objective function value RMSE = 9.84e-4, has fewer computational errors than other algorithms. Below the ACO, there are the algorithms GGHS and IGHS performing better in reducing the objective function value compared with other algorithms. In figure 5, a comparison has been made among the results obtained from different algorithms in finding the single-diode model of solar cells. It should be noted that the results obtained by other algorithms are in reference [19].

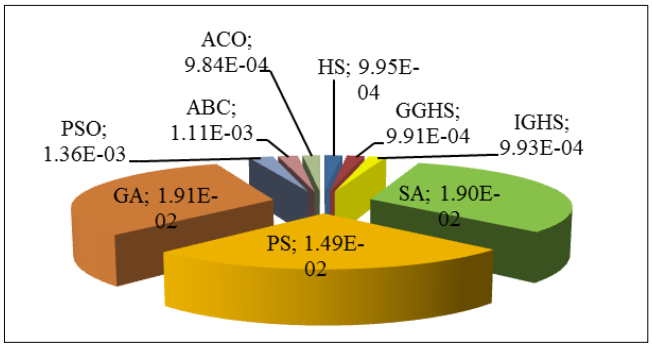

Fig 5: The RMSE Values Corresponding to Different Algorithms in the Single-Diode Model

5-3- Optimization of the Two-Diode Model of Solar Cells

In this part, a more precise model of the solar cell- the two-diode model- is to be studied. To get better results, the algorithm was performed 20 times and some best results have been recorded. It should be noted that the results of these 20 times were almost the same and the difference between the Worst and the best responses was 2e-4. The best response- achieved from the ant colony algorithm- is presented as the final result in table 5, along with the results of several other algorithms. The results of the single-diode model by other algorithms are presented in the reference [19].

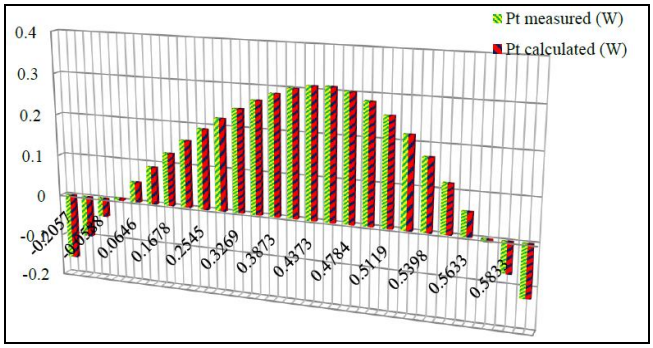

Fig 6: The Output Power of Solar Cells Obtained from Measurement and Simulation in the Single-Diode Model

5.3 Optimization of the Two-Diode Model of Solar Cells

In this part, a more precise model of the solar cell- the two-diode model- is to be studied. To get better results, the algorithm was performed 20 times and some best results have been recorded. It should be noted that the results of these 20 times were almost the same and the difference between the worst and the best responses was 2e-4. The best response- achieved from the ant colony algorithm- is presented as the final result in table 5, along with the results of several other algorithms. The results of the single-diode model by other algorithms are presented in the reference [19].

Table 5: The Results of Different Algorithms in the Two-Diode Model of Solar Cells

	R_s	R_{sh}	I_{ph}	I_{sd1}	I_{sd2}	*n1*	*n2*	*RMSE*
HS	0.3545	46.82696	0.76176	0.12545	0.2547	1.49439	1.49989	1.26E-03
GGHS	0.03562	62.7899	0.76056	0.37014	0.13504	1.49638	1.92998	1.07E-03
IGHS	0.0369	56.8368	0.76079	0.9731	0.16791	1.92126	1.42814	9.86E-04
SA	0.0345	43.1034	0.7623	0.4767	0.01	1.5172	2	1.66E-02
PS	0.032	81.3008	0.7602	0.9889	0.0001	1.6	1.192	1.52E-02
GA	0.0334	87.3984	0.7628	0.6377	0.36732	1.5594	1.8673	2.64E-03
PSO	0.03129	81.17952	0.761731	0.96344	0.96344	1.602342	1.61963	0.002527
ABC	0.0351	69.7899	0.7606	0.10727	0.51482	1.435	1.62	1.20E-03
ACO	0.0367	56.1965	0.7608	0.63683	0.23898	1.9986	1.46	9.82E-04

In the two-diode model of solar cells as well, the response received from the proposed ant colony algorithm has a lower RMSE than other algorithms. According to table [5], it is clear that the ant colony algorithm with RMSE = 9.82e-4 gives the best responses of all the other methods, and below that, IGHS and GGHS give better responses compared with other methods. The objective function values (RMSE) of various algorithms are compared with each other in figure 7.

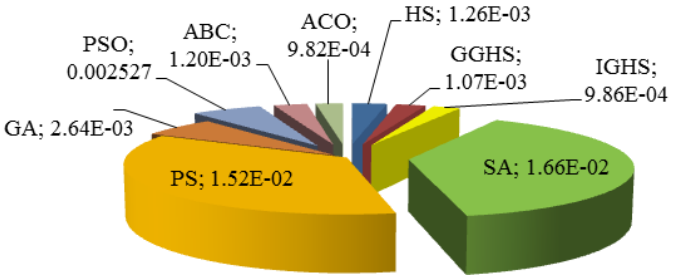

Fig 7: The Objective Function Values (RMSE) of Various Algorithms in the Two-Diode Model

After obtaining the two-diode model of the solar cell by ant colony algorithm, a comparison has been made between the measurement and simulation results. To do this, the voltage-power curve of the solar cell for the two-diode model is shown in figure (8).

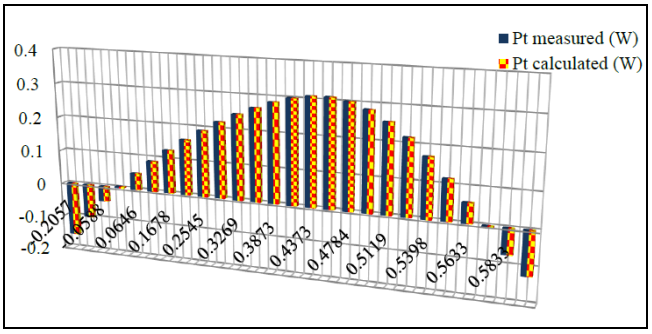

Fig 8: The Power Output of Solar Cells Obtained from Measurement and Simulation in the Two-Diode Model

5.4 The Solar Cell Maximum Power Point

After measuring a precise model of solar cells, we are going to calculate its maximum power. ACO algorithm has given a more appropriate solution than other algorithms and has been able to propose a precise model of both models of solar cells. Later in this chapter, maximum power values for both single and two-diode models will be measured in different situations and a comparison will be drawn between the two models. The maximum power values in experimental conditions for two models of solar cells are summarized in table (6). It is seen that the two values obtained are nearly close to each other. The reason is the high accuracy of the ant colony algorithm in finding the single and two-diode models of solar cells. Although the maximum power values obtained are quite identical, it should be born in mind that the maximum power value of the two-diode model is more precise and so close to the one obtained from the real test.

Table 6: The Coordinates of the Maximum Power Points of Solar Cells

	V_t (v)	I_t (A)	P_{out} (w)
The Single-Diode Model	0.4464	0.6680	0.2982
The Two-diode Model	0.4573	0.6781	0.3101
Measurement	0.4590	0.6755	0.3103

To get the maximum power value of solar cells at different temperatures and in various radiations, that model which depends on these two parameters should be used. The generated current of the solar cell model (I_{ph}) can be calculated by relation (15).

$$I_{ph} = \frac{S}{S_{ref}}\left[I_m^{ref} + \alpha(T - T_{ref})\right] \quad (15)$$

In equation (15), S is the radiation rate, S_{ref} is the radiation rate in standard conditions, T is the cell temperature at the operating point, T_{ref} is the temperature in standard conditions, α thermal coefficient of photovoltaic flow, and I_m^{ref} is the current in standard conditions. Diode current I_D can be achieved by equation (16):

$$I_D = I_0\left[e^{\frac{V_D}{nV_T}} - 1\right] \quad (16)$$

In relation (16), I_0 is the reverse saturation current, n is the idealization coefficient of the diode, and V_T is the thermal voltage calculated by equation (17):

$$I_D = I_0\left[e^{\frac{V_D}{nV_T}} - 1\right] \quad (17)$$

In relation (17), K is the Boltzmann's constant equal to $1.38^{\times}10^{-23}$J/K, q is the initial load equal to $1.6^{\times}10^{-19}$, and T, is the temperature in Kelvin scale. Diode reverse saturation current I_0 is strongly dependent on temperature and can be calculated from equation (18):

$$I_0 = I_0^{ref}\left[\frac{T}{T_{ref}}\right]^2 e^{\frac{E_G}{n}\left(\frac{1}{V_T^{ref}} - \frac{1}{V_T}\right)} \quad (18)$$

In equation (18), I_0^{ref} is the reverse saturation current in standard conditions of temperature and radiation, E_G is the silicon energy gap value equal to 1.12 eV, and, V_T^{ref} is the thermal voltage at a standard temperature. It should be noted that in equation (18) the temperature is in Kelvin scale. The current equation will be:

$$I_t = \frac{S}{S_{ref}}\left[I_t^{ref} + \alpha(T - T_{ref})\right] - I_0\left[e^{q\left(\frac{V_t + R_S I_t}{vkT}\right)} - 1\right] - \frac{V_t + R_S I_t}{R_{sh}} \quad (19)$$

Using the tested relations and the optimized parameters of solar cells, solar cell characteristics can be obtained at any other temperature and radiation. Entering the values of heat and solar radiation rate, voltage-current and voltage-power characteristics of solar cells, as well as MPP, can be obtained at any particular temperature and in any specific radiation rate. The voltage-power characteristic of the solar cell modeled in this thesis, at testing temperature (33 ° C) and in radiation rates of 1000, 800, 600 and 400, is drawn in figure 9. By a rise in the radiation rate, I_{sc} also increases and consequently, the output current of the solar cell increases leading to a rise in output power. An increase in radiation also leads to a rise in power and thus the amount of MPP also rises. In figure 9, the blue continuous line is for the two-diode model and the red dashed line is for the single-diode system. The maximum power of the solar cell in the two-diode model is more than the other model and its results are more precise as well. The maximum solar cell power points in various radiations are shown in the bar graph figure (10).

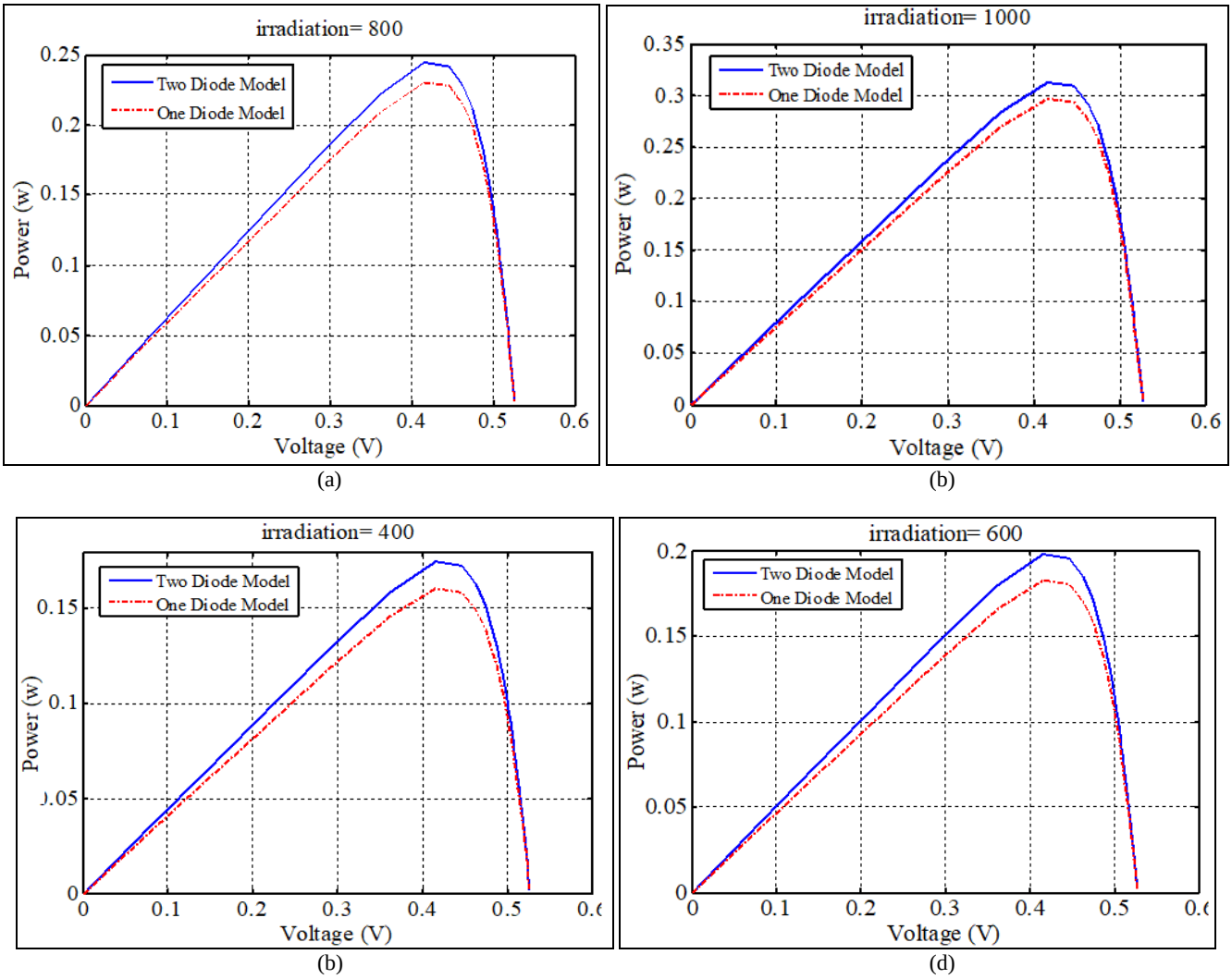

Fig 9: The Voltage-Power Characteristic of the Solar Cell Studied in Various Radiations

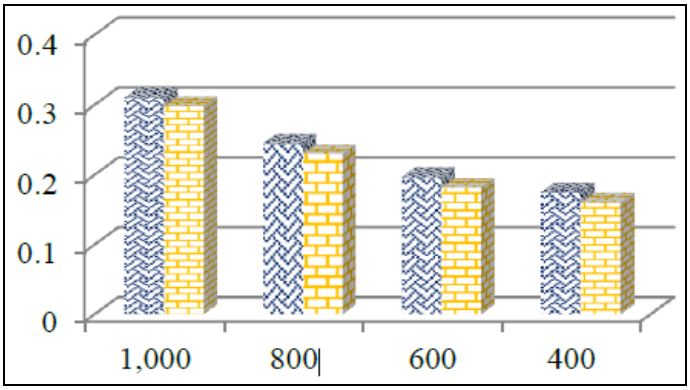

Fig 10: The Maximum Solar Cell Power in the Two Models in the Case of Different Radiation Rates

By reducing the temperature, the current and also the power of solar cells increase accompanied with an increase in MPP. The voltage-power characteristic of the solar cell with changes in temperature is plotted in figure (11). By studying the results obtained, it can be said that the two-diode model has a higher amount of MPP than the single-diode one. The two-diode model is of higher accuracy as well. For making more accurate comparisons, the maximum power values at different temperatures are shown in the bar graph figure (12).

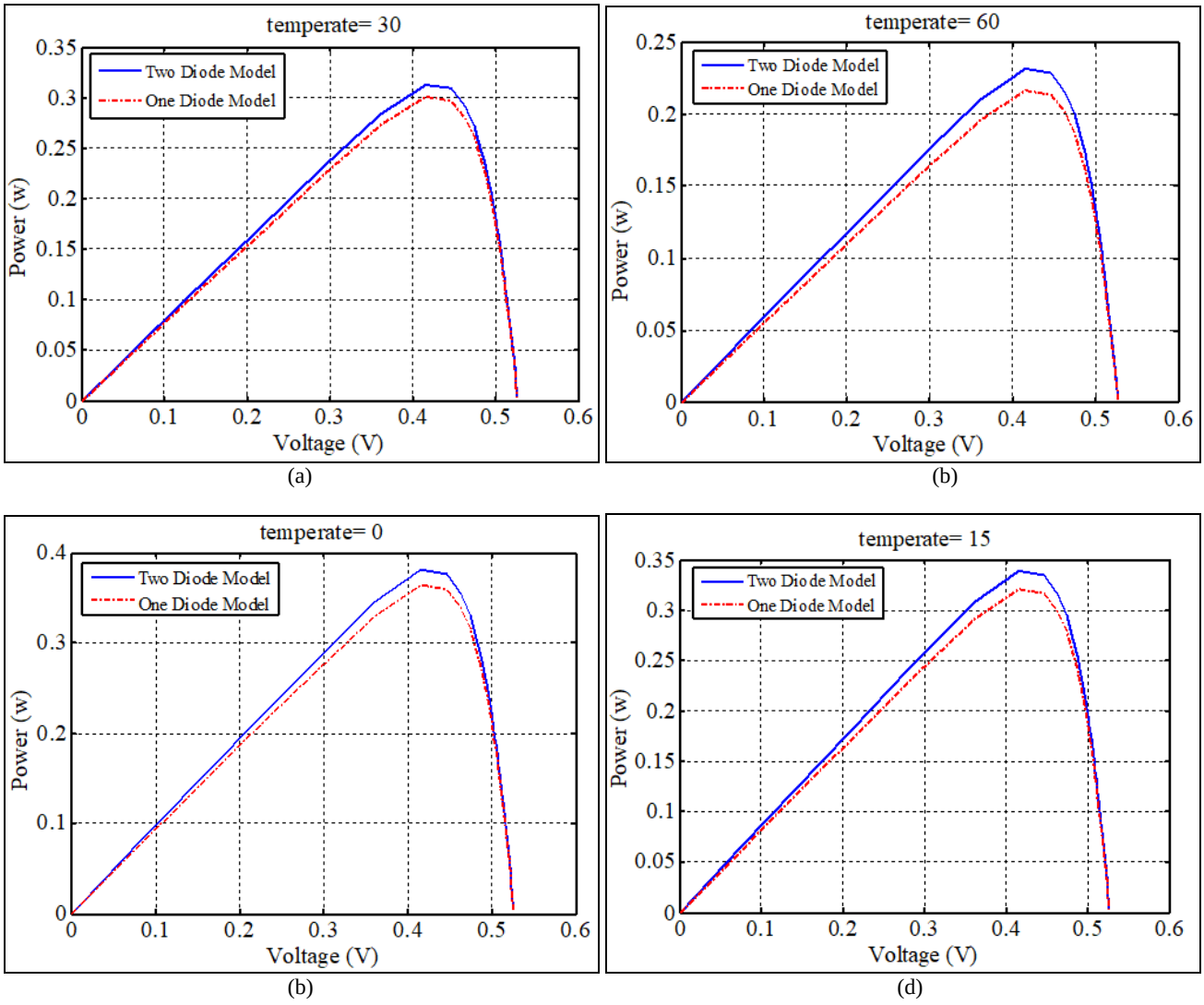

Fig 11: The Voltage-Power Characteristic of the Solar Cell Studied in Terms of Change in Temperature.

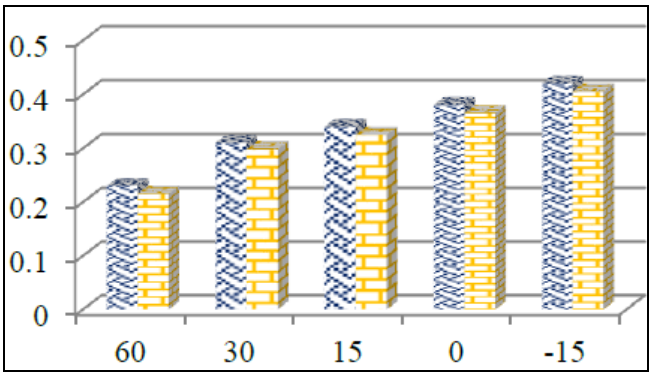

Fig 12: The Maximum Power Values of the Solar cell in the Two Models in Terms of Temperature Changes

6. Conclusion

In this paper, optimum design of single and two-diode models of solar cells has been studied. To do this, the powerful ACO algorithm was brought into use. The modeling was performed by taking the objective function (RMSE) into account. According to the simulation results, it can be said that in finding the precise parameters of solar cells, the ACO algorithm is more precise than other algorithms presented. The slight difference between the amount achieved in the real test and the one obtained by the use of algorithm was mostly due to the errors in recording the actual test results and also the approximations of the models used. In other words, if we record the practical results more precisely and find a better model for solar cells, then the RMSE amount can be reduced very much. Indeed, the results gained of solar cell parameters are reliable for modeling solar cells. If, one day, the results improve, the findings of this article will be still useful. For example, MPP will not change that much compared to the present coordinates. However, there are still ways to improve the present solutions by the use of new methods and algorithms. It's also necessary to say that providing a new model for solar cells, with regard to complexities it causes for calculations, is not an excellent solution for reducing errors compared with an increase in accuracy of practical test results. In addition, for applications other than MPP, the results of solar cell parameters obtained from the ACO algorithm can be used. Moreover, according to the results achieved from the single and two-diode models of solar cells, it can be said that these two models have produced quite identical results and

they are almost of the equal precision. The reason of this lies beneath the high precision of the algorithm in finding the optimal values of parameters. The RMSE values for the single and two-diode models are respectively 9.84E-04 and 9.82E-04. In spite of the slight difference, the difference in the solar cell maximum power points is a considerable one and it will increase if the number of cells are increased.

7. References

1. El-Naggar KM, AlRashidi MR, AlHajri MF, Al-Othman AK. Simulated annealing algorithm for photovoltaic parameters identification. Sol Energy. 2012; 86:266-74.
2. Jain S, Agarwal V. Comparison of the performance of maximum power point tracking schemes applied to single-stage grid-connected photovoltaic systems. IET Electr Power Appl. 2007; 1(5):753-62.
3. Noguchi T, Togashi S, Nakamoto R. Short-current pulse-based maximum-power-point tracking method for multiple photovoltaic-and converter module system. IEEE Trans Ind Electron. 2002; 49(1):217-23.
4. Masoum MAS, Dehbonei H, Fuchs EF. Theoretical and experimental analyses of photovoltaic systems with voltage and current-based maximum power-point tracking. IEEE Trans Energy Convers. 2002; 17(4):514-22.
5. Elgendy MA, Zahawi B, Atkinson DJ. Assessment of perturb and observe MPPT algorithm implementation techniques for PV pumping applications. IEEE Trans Sustainable Energy. 2012; 3(1):21-33.
6. Femia N, Petrone G, Spagnuolo G, Vitelli M. Optimization of perturb and observe maximum power point tracking method. IEEE Trans Power Electron. 2005; 20(4):963-73.
7. Mamarelis E, Petrone G, Spagnuolo G. A two-steps algorithm improving the P&O steady state MPPT efficiency. Appl Energy. 2014; 113:414-21.
8. AlRashidi MR, AlHajri MF, El-Naggar KM, Al-Othman AK. A new estimation approach for determining the I–V characteristics of solar cells. Sol Energy. 2011; 85:1543-50.
9. Fermia N, Granozio D, Petrone G, Vitelli M. Predictive & adaptive MPPT perturb and observe method. Aerospace Electron Syst, IEEE Trans. 2007; 43:934-50.
10. Ahmed J, Salam Z. An improved perturb and observe (P&O) maximum power point tracking (MPPT) algorithm for higher efficiency. Applied energy. 2015; 150:97-108.
11. Sera D, Mathe L, Kerekes T, Spataru SV, Teodorescu R. On the perturb-and-observe and incremental conductance MPPT methods for PV systems. IEEE Journal Photovoltaic. 2013; 3(3):1070-8.
12. Kjaer SB. Evaluation of the 'Hill Climbing' and the 'Incremental Conductance maximum power point trackers for photovoltaic power systems. IEEE Trans Energy Convers. 2012; 27(4):922-9.
13. Safari A, Mekhilef S. Simulation and hardware implementation of incremental conductance MPPT with direct control method using cuk converter. IEEE Trans Ind Electron. 2011; 58(4):1154-61.
14. Liu F, Duan S, Liu F, Ba Liu, Kang Y. A variable step size INC MPPT method for PV systems. IEEE Trans Ind Electron. 2008; 55(7):2622-8.
15. Wei H, Liu J, Yang B. Cost-benefit comparison between Domestic Solar Water Heater (DSHW) and Building Integrated Photovoltaic (BIPV) systems for households in urban China. Appl Energy. 2014; 126:47-55.
16. Esram T, Chapman PL. Comparison of photovoltaic array maximum power point tracking techniques. IEEE Trans Energy Convers. 2007; 22(2):439-49.
17. Dorigo M, Blum C. Ant colony optimization theory: a survey. Theor Comput Sci. 2005; 344:243-78.
18. Blum C. Ant colony optimization: introduction and recent trends. Phys Life Rev. 2005; 2(4):353-73.
19. Askarzadeh Alireza, Rezazadeh Alireza. Parameter identification for solar cell models using harmony search-based algorithms. Sol Energy. 2012; 86(11):3241-9.